Turkish Journal of Engineering
https://dergipark.org.tr/en/pub/tuje
e-ISSN 2587-1366

A Comprehensive Study of Microstructure and Mechanical Properties in Friction Stir Welded AA 2024 and Nano particle Reinforced Hybrid Composites

N. Mathan Kumar [1*], R.Suresh Kumar[2], Kundan Bharti[3], P. V. Nandhakumar[4], M.Yuvaperiyasamy[5]

[1*]*Centre of Machining and Materials Testing, KPR Institute of Technology, Coimbatore, Tamil Nadu, India, e-mail: mathannagarajbe@gmail.com*
[2]*Professor, Center for Advanced Material and Testing (DST-FIST Sponsored), Sri Eshwar College of Engineering, Coimbatore, India, e-mail : rsk777mech@gmail.com*
[3]*Department of Mechanical Engineering, Thakur College of Engineering and Technology (TCET), Mumbai, MH-India, e-mail: kundan.bharti@tcetmumbai.in*
[4]*Assistant professor, Department of Automobile Engineering, Karpaga Vinayaga College of Engineering and technology, Maduranthagam, Chennai, Tamilnadu, India, e-mail : pvnandha@gmail.com*
[5]*Saveetha School of Engineering, Saveetha Institute of Medical and Technical Sciences, Chennai, 602105, India, e-mail: yuvaperiyasamyvsb@gmail.com*

Cite this study: Mathan Kumar, N., Suresh Kumar, R., Kundan Bharti., Nandhakumar, P V., & Yuvaperiyasamy, M. (2025). A Comprehensive Study of Microstructure and Mechanical Properties in Friction Stir Welded AA 2024 and Nano particle Reinforced Hybrid Composites. Turkish Journal of Engineering, 9(2), 313-322.

https://doi.org/10.31127/tuje.1572285

Keywords
Aluminium matrix composites
Friction stir welding (FSW)
Hardness
Tensile Strength
Dispersion
Taguchi method

Research Article

Received:24.10.2024
Revised:10.12.2024
Accepted:10.12.2024
Published:01.04.2025

Abstract

The hybrid metal matrix composites have been composed of the AA 2024 matrix, the Silicon Nitride (Si3N4), and Aluminium Nitride (AlN) particle reinforcements through stir casting route with various combinations such as 0,2,4,6 & 8 wt%. The hybrid composites were successfully welded by the friction welding process with the various input parameters. The input parameters are Tool Rotational Speed (RPM), welding speed (mm/min), and Axial force (L). In this investigation, the L25 orthogonal array was used to conduct experiments, and the mechanical and metallurgical investigations are taken. Finally, the reinforcement particles were distributed evenly in the matrix. After successful welding 8wt% reinforced sample achieved higher mechanical properties as well and the heat-affected zone and weldment area were investigated and found that the weld strength improved.

1. Introduction

In the current scenario, industries have been using Aluminium Matrix Composites (AMC) widely for their superior characteristics strength and weight ratio good resistance in corrosion and working in heat compared to unreinforced aluminium [1]. From this promising satisfaction with the physical and other properties AMCs are universally convenient for automotive and aircraft industries [2], [3]. AMCs can be fabricated by adding ceramic particles to obtain isotropic properties, resisting oxidation, involved in elevated temperature conditions, and for easy fabrication [4]. Typically, fusion-based techniques are used to fabricate the AMCs. By fabricating this fusion technique leads to some problems like unfavourable and non-homogeneous microstructure, tensile strength affected by the casting defects, blow holes' porosity, and inclusions. Meanwhile the main reason for restraining the growth of all the place in industries consuming AMCs because of the trustworthiness in fusion welding processes like Tungsten Inert Gas welding (TIG), Resistance welding, Laser beam welding, and Gas metal arc welding (GTAW),

etc., [5]. Instead, the commercial methods of welding in AMCs are difficult, and not get adequate welded strength in all aspects and are challenging as brittle in its second phase making the formation between the matrix and reinforcement particles [6]. Many researchers have done research on Friction Stir Welding for various heterogenous materials and analyzed the various joints made by various alloys, additionally in this investigation reveals information about the different grades of aluminium alloys [7-11].

In recent decades, many researchers accounted for investigated the effect of the parameters in FSW on the mechanical properties and metallurgical properties of 2xxx aluminum alloys as a base grid built up with different ceramic particles. In Solid-state welding, Friction Stir welding (FSW) is viewed as a reliable joining for AMCs. In the FSW, can achieve fine grains and even disbursed of reinforcements in the nugget zone by heat and plastic deformation in AMCs. In any case, it is not an easy task for FSW on MMCs having significant challenges in accomplishing ideal welding windows and adequate mechanical properties. In the FSW process, the rotation tool is used to make friction or contact between two plates and the rotating tool has the shoulder and pin inserted between the two plates. The material gets softened due to friction created a heat by the contact of the material and the tool. The stirring process is done by the rotational tool and simultaneous transverse motion of the tool, the composites get Complex movement and Severe Plastic Deformation (SPD). In continuation of the stirring the material has uniform friction, forging action, and extrusion. Whereas the terminologies used in the tool rotation are FSW, and the transverse is the same as the advancing side. (AS), another side is called the Retreating Side (RS), Heat Affected Zone (HAZ), Stir or Nugget Zone (NZ), and Thermo-Mechanically Affected Zone (TMAZ) are the three distinct zones.

Many researchers have done their research on FSW on dissimilar aluminium alloys [12], [13]. It is simpler to decide the place of examinations in dissimilar joints can yield additional information about joints formed of different metals. In previous research, different series of aluminium alloys are welded successfully and examined, i,e. AA2xxx & AA6xxx, AA5xxx & AA7xxx [14-19]. It has been found that the mechanical properties and microstructures of FSW joints impact process parameters. [10], have analyzed the result of the rotational speed of the tool on the AA6061-7050 joint's microstructure and mechanical properties, Results demonstrate by [12] that the internal mixing degrees on the cross-section of the weld joints are related to tool rotation speed and that weld strength improves with increasing speed. studied that the welding speed is influenced by the speed of tool rotational on the residual stresses on AA5083-6082 welded joints, the residual stresses can be optimized by adjusting the tool rotational speed. Suresh S., et.al observed that the speed of tool rotation significantly affected the heat generation of the joint, from tool rotational speed plays an important role in FSW process. Besides, a few examinations have been devoted to investigating the dissimilar materials FSW processes of AA7xxx and 2xxx [20], yet most of them were restricted to a tight scope of process parameters. In this way, more orderly investigations are yet required for better comprehension of the microstructure examination and mechanical characteristics of the weld joints with various tool rotational speeds.

In this investigation, AA 2024 material was used as a matrix and Silicon Nitride (Si3N4), Aluminium Nitride (AlN) were selected as reinforcements. The AMC has been made by stir casting method with (0, 2, 4, 6 &8) wt% of reinforcements. The mechanical and metallurgical investigation has been done in the heat-affected zone and weld zone in samples to identify the influence of reinforcement particles.

2. Materials preparation and Experiments

2.1 Preparation of AA 2024 AMC

AA 2024 provides a high strength-to-weight ratio, excellent heat absorption, and good corrosion resistance, making it ideal for applications in aerospace and automotive industries where lightweight and durability are essential.In this article, AA 2024 was used as the matrix due to its high heat absorption and maintaining strength, chemical composition, and Silicon Nitride (Si3N4) and Aluminium Nitride (AlN) ceramic particles are selected as the reinforcements. The AA 2024 AMC is prepared by a simple and effective stir-casting method. The 0, 2, 4, 6,8wt% of reinforcements are added with the AA 2024 molten metal. The stirring action helps the reinforcements to evenly disperse in the matrix. The molten mixture of the matrix and reinforcements have been poured into the 50mm × 50mm and 5mm thickness pre-prepared cavity and allowed to solidify.

2.2 Friction Stir Welding (FSW)

In FSW, the external bimetallic tool is used to make a weld, the tool is prepared with tool steel (D3) shoulder, and the tool pin was made up of Grade 5 titanium. The tool material has a higher wear resistance and higher hardness in elevated temperature conditions. The tool was further hardened with oxy-acetylene flame followed by oil quenching. The shoulder diameter is 12mm and the of the pin diameter is 4mm. The pin length was 1.5mm. For making a weld a high rigid machine was used, and the parameters are selected. The tool rotation speed (RPM) has changed from 400, 600, 800, 1000 and 1200rpm respectively. The welding speed is constantly maintained at 50mm/min and the axial force was 1500kg [30].

2.3 Specimen Testing

The welded specimens were used to find mechanical properties such as Micro Vickers's Hardness and Tensile testing as per ASTM standards. The tensile strength done by Universal Testing Machine (UTM) as per ASTM E08-08. The samples were polished with 1200 grade emery sheets used to clean the surface from dust particles and achieve better capture. The load of 10 KN is applied to carry the test with 2.5m/min cross head speed. The hardness of the welded samples was determined in several regions of the weldment area for obtaining the average value as per the ASTM E10-07 standard. The hardness test was done with room temperature condition and the load applied 0.5 kg with the time of 15 seconds. Microstructural investigations have been made such as Microstructure, Scanning Electron Microscope

test (SEM) for identifying structural and phase changes takes place in weld interface and the presents of metallic elements.

2.4 Optimization Techniques

2.4.1 Taguchi Method

The L25 orthogonal array was used to systematically vary process parameters, allowing the study to identify the most influential factors on mechanical properties with fewer experiments, saving time and resources while effectively optimizing the welding process. Taguchi the famous quality engineer from Japan, worldwide recognized as the father of quality engineering. Taguchi has two main quality methods: offline and online quality method. The Taguchi tool is a powerful problem-solving method that is used to enhance the process, design, and product performance with minimum cost and time. The number of experiments has increased due to the increment of process parameters. Due to this complexity, to sort out the problem Taguchi method has an orthogonal array for designing experiments. Moreover, the Taguchi method can reduce the fluctuation of system and quality performance in the source of variation [31].

Basic steps can be followed in Taguchi method are,

1. Find out the quality characters and performance parameters of the experiment.
2. Select the appropriate orthogonal array with assigning the parameters with condition of Lower is Better, Nominal is Better and Larger is better.
3. Experiments done with the base of an orthogonal array.
4. Analyze the results with Signal to Ratio (S/N) and Analysis of Variance (ANOVA).
5. Making the decisions with the parameters influencing the experimental results.

3 Results and Discussions

3.1 Micro Vicker's Hardness Test Results

Hardness was highest in the nugget zone due to fine grain refinement and the effectiveness of particle dispersion. The heat-affected zone (HAZ) displayed lower hardness as it experienced less intense plastic deformation and particle distribution. The highest hardness values were observed in the NZ due to fine grain refinement and optimal reinforcement dispersion. The HAZ and TMAZ exhibited lower hardness levels as they experienced less mechanical agitation and reinforcement effects. Figure 1 Shows the Hardness results for the various wt% of reinforcements and different rotational speeds of composites. The hardness values can be focused on the weldment area (stirring zone) for identifying the hardness level in joints. The lower hardness values were observed in all wt% of reinforcements in increasing the speed of the tool. The profile of the weldment area exhibits the asymmetric distribution of grains in all combinations. According to the welding parameters, the sample softens while stirring, and increasing the heating in the stirring zone the hardness is higher in base metal [21-23]. At the higher speed, the stirring zone got a fine refinement during welding. Hence, the heat-affected zone and the base metal have a lower value of hardness. In the FSW process, the thermal cycles are developed and it causes the dissolution and coarsening of hardening precipitates the result of hardness in the weldment area. The increment of tool rotational speed precipitates the distribution of particles which increased the hardness. And other term the higher tool rotation speeds are the key to increasing the heat development in the friction zone (Weldment area) the reinforcements were pushed up from the matrix and interchanged between the two materials. Among the welded samples the increment of hardness has been found in the increment of reinforcement and decrement of tool rotational speed.

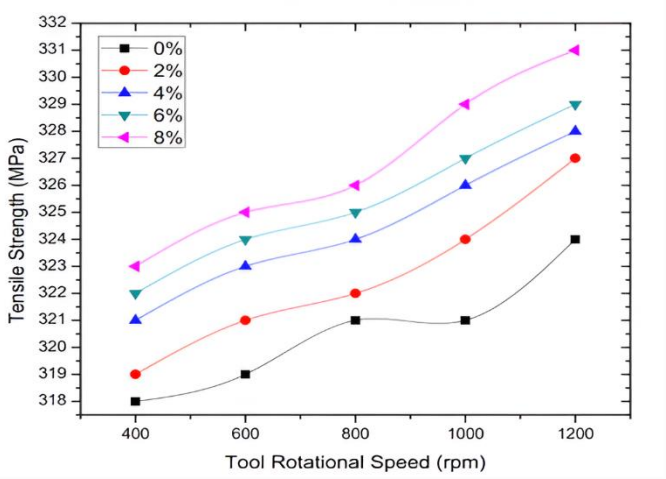

Figure 2. Tensile results of various wt% of reinforcements of welded samples

From the Hall – Petch relationship theory the hardness can be increased with the fine grain refinement and distribution. In addition, the accelerated dispersion gave a strong influence on the hardness esteems in examination with grain size effect in the weld.

3.2 Ultimate Tensile Test Results

Figure 2 shows the tensile results of various wt% of reinforcements of composites and various tool rotational speeds. The ultimate tensile tests have been conducted for each sample. The higher tensile strength has been obtained for higher tool rotational speed and higher wt% of reinforcement. The lower tensile strength has been identified for the lower rotational speed of samples. The lower tool rotational speed made an insufficient heat input, and the weld was not done properly, due to the lack of heat input in the stirring zone grain transformation was not proper. Pin hole and tunnel effects have been identified in the stirring zone due to lack of sufficient heat input [24], [25]. From the tested samples the reinforcement wt% is varied and the sample gets fractured in different locations. The lower wt% of reinforcements are dispersed in the matrix evenly but the higher wt% of reinforcements possibly to dispersed maximum level in the matrix. The load can be transferred through reinforcement and influenced to get higher strength. Mainly the fracture locations were found in Heat heat-affected zone (HAZ) and thermo-mechanically affected zone (TMAZ). When the tool rotational speed has been increased, it tends to move HAZ and Base material

(BM). Nugget Zone has equalized fine grains, the failure of elongation has been found in low wt% of reinforcements and low tool rotational speed due to insufficient grain transformation. In contrast, a high wt% of reinforcement and tool rotational speed sample exhibits higher ductility. Moreover, the higher reinforced welded sample has a continuous yielding and identified yielding the serration called the "jerky flow" phenomenon. The higher tensile strength samples possess a finer grain size in the entire area. Under maximum FSW joints are subjected to welding conditions. Have shear fractures occurred in HAZ. The lower tensile strength produces micro defects due to low fine refinement, lack of heat input and lack of grain transformation between the joints. By raising the rotating speed of the tool, the high heat generated and the stirring and transformation of grains effectively to obtain the higher hardness and tensile properties.

3.3 Microstructural Evaluation

Higher rotational speeds lead to more heat generation, which refines grains in the NZ and improves particle distribution. This results in increased hardness and tensile strength, while lower speeds can result in inadequate heat input, leading to coarser grains and potential defects. Microstructure evaluation has been done for the FSW welded samples with various reinforcements and parametric combination. It can be clearly noticed that the reinforcements are evenly dispersed in the matrix. It is observed that the maximum wt% of reinforcements and high tool rotational speed combinations has fine surface roughness when compared to other parameters. In Fig.4 shows that during welding the maximum flash out with compared the other samples got in better surface finish. The maximum tool rotational speed combination an inordinate measure of flash expelled out of the weld zone during welding. In micrographs exhibits the better grain refinement after welded, due to the high heat generation during welding at high tool rotational speed the particle has transferred as fine grains. Figure.4 shows the homogeneous distribution of Si3N4 and AlN particles in stirring zone. Commonly, there are no major differences in particle uniformity in Base Material and Nugget zone. In the micrographs marked that the lesser concentration in nugget zone compared with base material. The behavior of reinforcements is more articulated for the composite with 8% of Si3N4 and AlN, because of its generally higher measure of molecule groups. As a result, a defect-free joint may be attained at a high rotating speed of 1200rpm. During welding the tool rotates at high speed and the heat generated produces with strong interlocking of AA2024 matrix with Si3N4 and AlN reinforcements. The shapes of matrix anchors constantly change according to the change of tool rotational speed with respect to change of stirring ability and heat input. The lower tool rotational speed does not have sufficient heat input and stirring to breaking the ability of the Al anchors into pieces, instead of that, the increasing of tool rotational speed has sufficient heat input and tool rotational speed can able to break the Al anchors into small pieces for getting fine particles after getting welded. While the sample getting higher tool rotational speed of 1200 rpm the weldment area got softened and causes bending and elongation of the matrix with the limited level by relatively minimum and wiper shape. In microstructure shows that during joining with the high tool rotational speed there is no evidence found that interfacial bonding defects. The interfacial bonding defects such as cracks and bubbles can be avoided with the help of high thermal conductance and maximum forging force during welding. Finally, the microstructure reveals the better dispersion between AMC joints during high tool rotational speed the transformation of particulates has the strong bonding in the weldment evident to increasing the micro hardness and tensile strength of the welded samples.

3.4 Scanning Electron Microscope Evaluation

SEM images showed a uniform distribution of reinforcement particles in high-speed welded samples, with minimal defects like cracks or voids. This suggests that increased tool rotation speeds promote better bonding and dispersion of particles within the matrix. Figure 4 shows the SEM images for various tool rotational speed welded samples. The surface morphologies of welded samples with various wt% of reinforcements and tool rotational speeds reveal that the lower tool rotational speed welded sample has a rough surface formation, because of its insufficient heat input. High tool rotational speed has a smoother surface due to its high heat while high-speed friction. The welded joint shows the nonstop flow of plasticized material between AS and RS. The weldments are free from volume imperfections like pin holes and tunnels formed in deep penetration under all welding conditions. With sufficient heat, stirring action and the plastic deformation of the material indicate uniform plasticization and flow of the material in proper coalescence. However, the macro defects seen on the top surface, which related to the pullout in the nitride layer. To determine the effect of various wt% of reinforcements and tool rotational speed on the fine dispersion rate [26], [27]. On the closed magnifying on the samples AMC has the fine distribution of reinforcements and uniform grain structure. Another interesting finding was varied significantly in nugget zone at various tool rotational speeds. This appearance is called onion rings and it was commonly found in Friction Stir welded aluminium alloys. During stirring of the welding, the tool travel traces have been recorded and that have been considered as onion rings. This is in concurrence with the way that the onion-ring structure may be the geometric effect.

4.Optimization of Results

4.1 Taguchi Method

In this article, AA 2024 matrix and the Si3N4 and AlN have been reinforced with various weight percentages are 0%, 2%, 4%, 6% and 8%. The various wt% of reinforced samples were welded according to the L25 orthogonal array as shown in Table.1. From the Taguchi method Signal to Noise ratio and Analysis of Variance were analyzed [28], [29].

4.2 Signals to Noise Ratio

Figure 5 (a) & (b) graphs show that the DOE (Design of Experiments) exhibits the physical quantification to determine the process parameters for controlling the process by decreasing noise factors. The objective of describing the condition is larger is best to identify the maximum Hardness and Tensile strength. The various process parameters were used to weld the samples. Axial force and Weld speed have been kept constant and tool rotation speed has been increased for various wt% of reinforcements according to the design of the experiment. The Hardness and Tensile strength are analyzed with the process parameters and changed into mean and Signal to Noise ratio. From the analysis, the weld strength increases with the increment of wt% of reinforcement and tool rotational speed. From Signal to Noise ratio composites have the main influencing processing parameter for achieving the maximum Hardness and Tensile strength.

4.3 Analysis of Variance

Figure 5 (c) & (d) graphically represent the Analysis of Variance (ANOVA) is mainly used to identify the significant process parameters of the experiments. In this research AA 2024 AMCs with various wt% of reinforcements welded with 25 combinations of process parameters. Such an experiment which is most influencing or has the maximum contribution of the joint strength is analyzed. Illustrates the readings of Hardness of the composites for the adjacent sum of squares and Mean squares and the composite has the 71.89% contributing higher to achieve the maximum strength. Wt% of reinforcements evenly distributed with the matrix and bonding of each particle are good. Furthermore, tool rotational speed has the lowest contribution to achieve the maximum hardness.

In the case of Tensile strength, Tool rotational speed has the higher influencing process parameter 55.77% for achieving the maximum tensile strength. Composites have the lower contribution 42.68% because of tool rotation speed has higher friction in the maximum Wt% of reinforced samples and the molecules were interchanged between the samples [32].

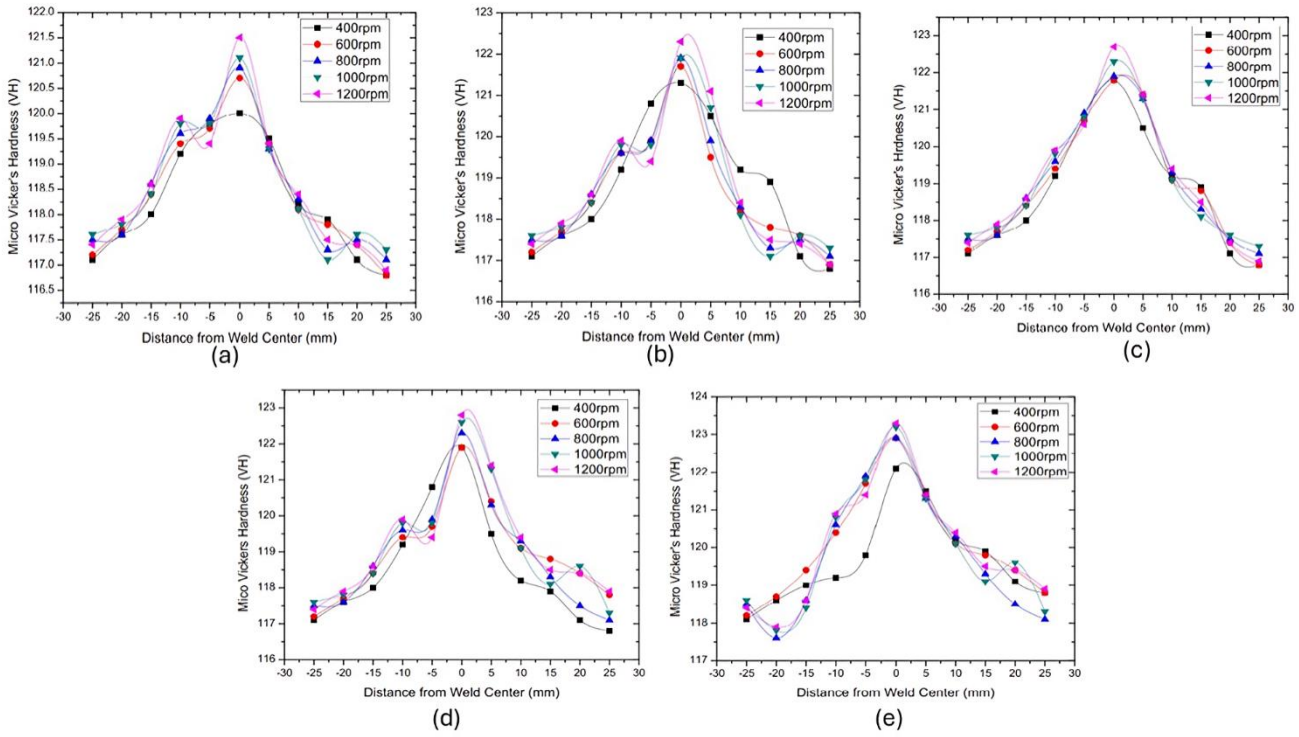

Figure 1. MicroVicker's Hardness results in various zones (a) 0%, (b) 2%, (c) 4%, (d) 6% and (e) 8%

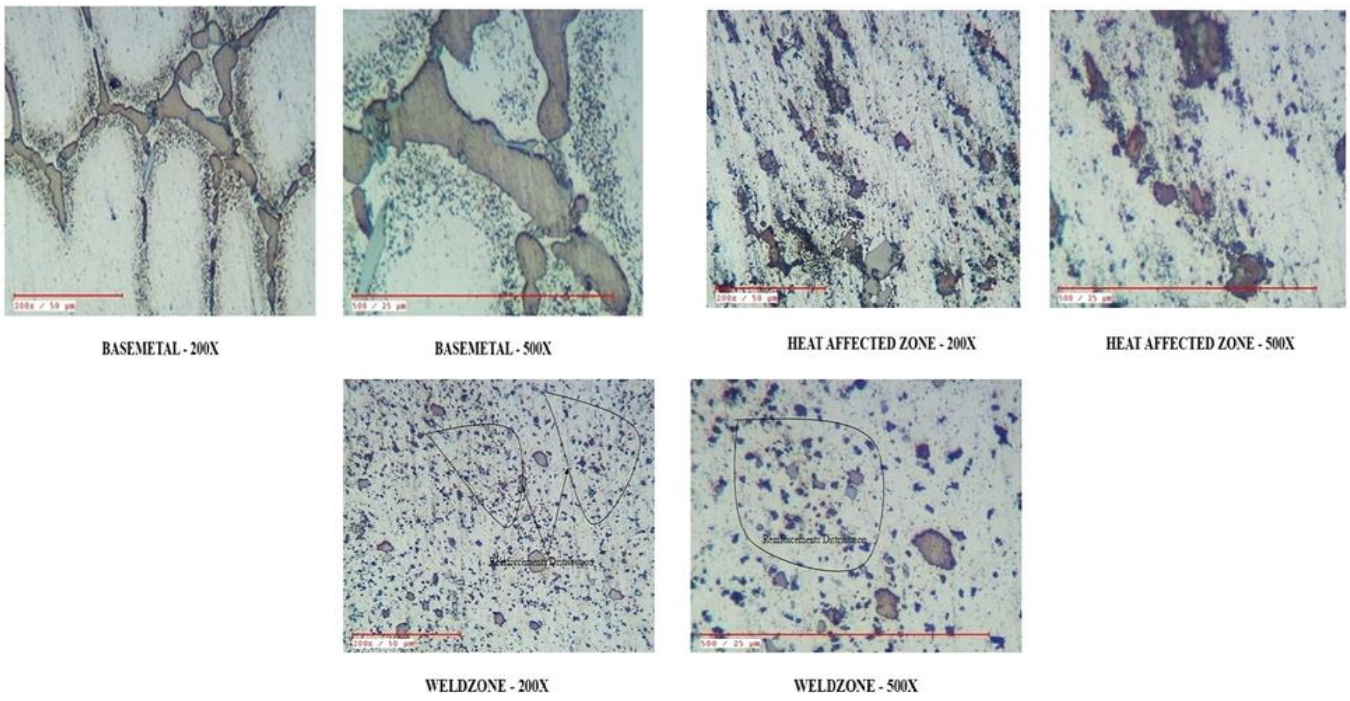

Figure 3. Microstructure images of 8wt% of welded sample with different zones

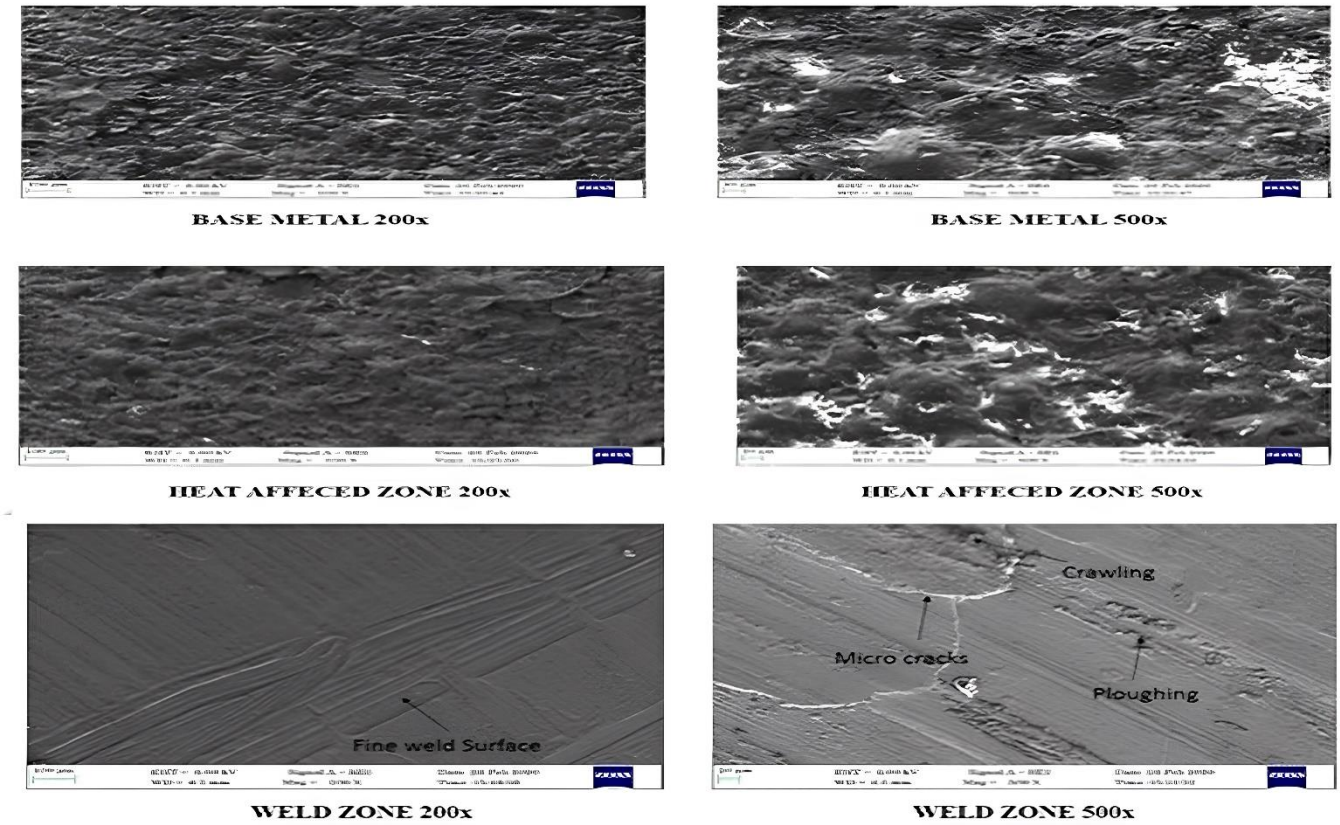

Figure 4. SEM images of 8wt% of welded sample

Table 1. L25 Orthogonal Array Tensile Strength (Mpa)

Sl.No	Composites (Wt% of reinforcements)	Welding Speed (mm/min)	Axial Force L (Kg)	Tool Rotational Speed (rpm)	Vickers Hardness (HV)	Tensile Strength (Mpa)
1	0	400	50	1500	120.0	318
2	0	600	50	1500	120.7	319
3	0	800	50	1500	120.9	321
4	0	1000	50	1500	121.1	321
5	0	1200	50	1500	121.7	324
6	2	400	50	1500	121.3	319
7	2	600	50	1500	121.7	321
8	2	800	50	1500	121.9	322
9	2	1000	50	1500	121.9	324
10	2	1200	50	1500	122.3	327
11	4	400	50	1500	121.8	321
12	4	600	50	1500	121.8	323
13	4	800	50	1500	121.9	324
14	4	1000	50	1500	122.3	326
15	4	1200	50	1500	122.7	328
16	6	400	50	1500	121.9	322
17	6	600	50	1500	121.9	324
18	6	800	50	1500	122.3	325
19	6	1000	50	1500	122.6	327
20	6	1200	50	1500	122.8	329
21	8	400	50	1500	122.1	323
22	8	600	50	1500	122.9	325
23	8	800	50	1500	122.9	326
24	8	1000	50	1500	123.2	329
25	8	1200	50	1500	123.3	331

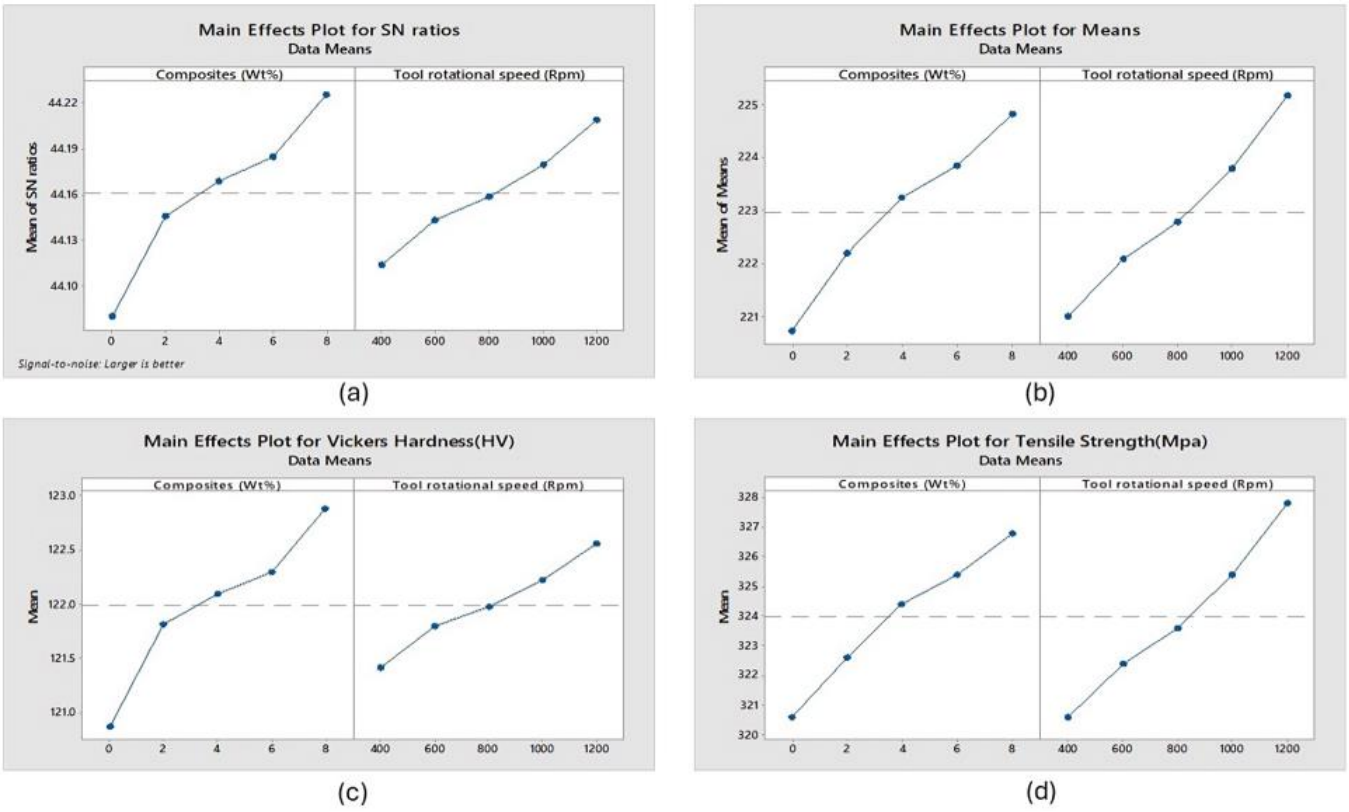

Figure 5. (a) Main Effects Plots for SN ratio, (b) Main Effects Plots for Means, (c) Main Effects Plot for Vickers Hardness, (d) Main Effects Plot for Tensile strength

5. Conclusions

- In this research article AA 2024 was selected as matrix and reinforcements as Silicon Nitride (Si3N4) and Aluminium Nitride (AlN). The reinforcements are blended with the matrix for the weight percentages like 0,2,4,6 and 8% through the stir casting method.
- In Composites the reinforcements are evenly distributed, and the particle bonding is good. This is evident from microstructures.
- In this research Friction welding method is used to weld the samples with various process parameters and the Taguchi method is used to optimize the welded joints. Using L25 orthogonal array was selected to weld the samples with the combination of various process parameters.
- The Vicker's hardness and tensile strength have been investigated. The hardness values focused on the weldment area (stirring zone) for identifying the hardness level in joints. The lower hardness values obtained in all wt% of reinforcements in increasing the tool rotational speed.
- In FSW process the thermal cycles are developed and it results in coarsening and disintegration of hardening collects resulting of hardness in the weldment area. The increment of tool rotational speed precipitates the distribution of particle has been increased the hardness. The maximal hardness was found in 8% sample with hardness value of 123.3HV for the 1200rpm of tool rotational speed.
- By incremental of tool rotational speed, the high heat is generated. Uniform stirring and transformation of grains yield the higher tensile strength of 331 Mpa.
- The welded samples are induced microstructural and SEM investigations. In microstructure of the weldment area has the good particle distribution and good bonding between two samples. Hence the defect free joint can be achieved at high rotational speed of 1200 rpm. During welding the tool rotates at high speed and the heat produces a that attribute with strong interlocking with AA2024 matrix and Si3N4 and AlN reinforcements.
- From SEM evaluation, the surface morphologies are evaluated of welded samples with various wt% of reinforcements and tool rotational speeds reveals that the lower tool rotational speed welded sample produces a rough surface formation, because of its insufficient heat input.
- During stirring of the welding, the tool travel traces have been recorded and that have been considered as onion rings. This is in concurrence with the way that the onion-ring structure may be the geometric effect.

- The composite has 71.89% contributing higher to achieve the maximum strength.
- In the case of Tensile strength, Tool rotational speed has the higher influencing process

Author contributions

N. Mathan Kumar: Conceptualization, Methodology, Software R. Suresh Kumar: Data curation, Writing-Original draft preparation, Kundan Bharti**:** Software, Validation. P. V. Nandhakumar: Visualization, M. Yuvaperiyasamy: Writing-Reviewing and Editing.

Conflicts of interest

The authors declare no conflicts of interest.

References

1. Prater, T. (2014). Friction stir welding of metal matrix composites for use in aerospace structures. Acta Astronautica, 93, 366–373.
2. Kumar, N. M., & Kumaraswamidhas, L. A. (2019). Characterization and tribological analysis on AA 6061 reinforced with AlN and ZrB2 in situ composites. Journal of Materials Research and Technology, 8(1), 969–980.
3. Chawla, K. K., & Chawla, K. K. (1998). Metal matrix composites. Springer.
4. Suresh, S. (2013). Fundamentals of metal-matrix composites. Elsevier.
5. Das, H., Mondal, M., Hong, S.-T., Chun, D.-M., & Han, H. N. (2018). Joining and fabrication of metal matrix composites by friction stir welding/processing. International Journal of Precision Engineering and Manufacturing Technology, 5, 151–172.
6. García, R., López, V. H., Kennedy, A. R., & Arias, G. (2007). Welding of Al-359/20% SiCp metal matrix composites by the novel MIG process with indirect electric arc (IEA). Journal of Materials Science, 42, 7794–7800.
7. Reynolds, A. P. (2000). Visualisation of material flow in autogenous friction stir welds. Science and Technology of Welding and Joining, 5(2), 120–124.
8. Threadgill, P. L., Leonard, A. J., Shercliff, H. R., & Withers, P. J. (2009). Friction stir welding of aluminium alloys. International Materials Reviews, 54(2), 49–93.
9. Çam, G., & Mistikoglu, S. (2014). Recent developments in friction stir welding of Al-alloys. Journal of Materials Engineering and Performance, 23, 1936–1953.
10. Guo, J. F., Chen, H. C., Sun, C. N., Bi, G., Sun, Z., & Wei, J. (2014). Friction stir welding of dissimilar materials between AA6061 and AA7075 Al alloys: Effects of process parameters. Materials and Design, 56, 185–192.
11. Chen, Y., Ding, H., Cai, Z., Zhao, J., & Li, J. (2017). Microstructural and mechanical characterization of a dissimilar friction stir-welded AA5083-AA7B04 butt joint. Journal of Materials Engineering and Performance, 26, 530–539.
12. Steuwer, A., Peel, M. J., & Withers, P. J. (2006). Dissimilar friction stir welds in AA5083--AA6082: The effect of process parameters on residual stress. Materials Science and Engineering A, 441(1–2), 187–196.
13. Peel, M. J., Steuwer, A., Withers, P. J., Dickerson, T., Shi, Q., & Shercliff, H. (2006). Dissimilar friction stir welds in AA5083-AA6082. Part I: Process parameter effects on thermal history and weld properties. Metallurgical and Materials Transactions A, 37, 2183–2193.
14. Cavaliere, P., De Santis, A., Panella, F., & Squillace, A. (2009). Effect of welding parameters on mechanical and microstructural properties of dissimilar AA6082-AA2024 joints produced by friction stir welding. Materials and Design, 30(3), 609–616.
15. Jonckheere, C., De Meester, B., Denquin, A., & Simar, A. (2013). Torque, temperature, and hardening precipitation evolution in dissimilar friction stir welds between 6061-T6 and 2014-T6 aluminum alloys. Journal of Materials Processing Technology, 213(6), 826–837.
16. Tan, Y. B., et al. (2017). A study on microstructure and mechanical properties of AA 3003 aluminum alloy joints by underwater friction stir welding. Materials Characterization, 127, 41–52.
17. Mehta, K. P., Carlone, P., Astarita, A., Scherillo, F., Rubino, F., & Vora, P. (2019). Conventional and cooling assisted friction stir welding of AA6061 and AZ31B alloys. Materials Science and Engineering A, 759, 252–261.
18. Wang, Q., Zhao, Z., Zhao, Y., Yan, K., & Zhang, H. (2015). The adjustment strategy of welding parameters for spray-formed 7055 aluminum alloy underwater friction stir welding joint. Materials and Design, 88, 1366–1376.
19. Moradi, M. M., Aval, H. J., Jamaati, R., Amirkhanlou, S., & Ji, S. (2018). Microstructure and texture evolution of friction stir welded dissimilar aluminum alloys: AA2024 and AA6061. Journal of Manufacturing Processes, 32, 1–10.
20. Tran, V.-X., Pan, J., & Pan, T. (2009). Effects of processing time on strengths and failure modes of dissimilar spot friction welds between aluminum 5754-O and 7075-T6 sheets. Journal of Materials Processing Technology, 209(8), 3724–3739.
21. Hasan, M. M., Ishak, M., & Rejab, M. R. M. (2017). Effect of backing material and clamping system on the tensile strength of dissimilar AA7075-AA2024 friction stir welds. International Journal of Advanced Manufacturing Technology, 91, 3991–4007.
22. Cole, E. G., Fehrenbacher, A., Duffie, N. A., Zinn, M. R., Pfefferkorn, F. E., & Ferrier, N. J. (2014). Weld temperature effects during friction stir welding of dissimilar aluminum alloys 6061-T6 and 7075-T6. International Journal of Advanced Manufacturing Technology, 71, 643–652.

23. Rodriguez, R. I., Jordon, J. B., Allison, P. G., Rushing, T., & Garcia, L. (2015). Microstructure and mechanical properties of dissimilar friction stir welding of 6061-to-7050 aluminum alloys. Materials and Design, 83, 60–65.
24. Bijanrostami, K., Barenji, R. V., & Hashemipour, M. (2017). Effect of traverse and rotational speeds on the tensile behavior of the underwater dissimilar friction stir welded aluminum alloys. Journal of Materials Engineering and Performance, 26, 909–920.
25. Giraud, L., Robe, H., Claudin, C., Desrayaud, C., Bocher, P., & Feulvarch, E. (2016). Investigation into the dissimilar friction stir welding of AA7020-T651 and AA6060-T6. Journal of Materials Processing Technology, 235, 220–230.
26. Aval, H. J. (2015). Influences of pin profile on the mechanical and microstructural behaviors in dissimilar friction stir welded AA6082-AA7075 butt joint. Materials and Design, 67, 413–421.[27] Selvaraj, S. K., Nagarajan, M. K., & Kumaraswamidhas, L. A. (2017). An investigation of abrasive and erosion behaviour of AA 2618 reinforced with Si3N4, AlN, and ZrB2 in situ composites by using optimization techniques. Archives of Civil and Mechanical Engineering, 17, 43–54.
28. Kumar, N. M., Kumaran, S. S., & Kumaraswamidhas, L. A. (2016). Wear behaviour of Al 2618 alloy reinforced with Si3N4, AlN, and ZrB2 in situ composites at elevated temperatures. Alexandria Engineering Journal, 55(1), 19–36.
29. Kumar, N. M., Kumaran, S. S., & Kumaraswamidhas, L. A. (2016). High temperature investigation on EDM process of Al 2618 alloy reinforced with Si3N4, AlN, and ZrB2 in-situ composites. Journal of Alloys and Compounds, 663, 755–768.
30. Kaygusuz, E., Karaomerlioglu, F., & Akinci, S. (2023). A review of friction stir welding parameters, process, and application fields. Turkish Journal of Engineering, 7(4), 286–295. https://doi.org/10.31127/tuje.1107210
31. Kahraman, F., & Sugözü, B. (2019). An integrated approach based on the Taguchi method and response surface methodology to optimize parameter design of asbestos-free brake pad material. Turkish Journal of Engineering, 3(3), 127–132. https://doi.org/10.31127/tuje.479458
32. Buldum, B. B., & Cagan, S. C. (2017). The optimization of surface roughness of AZ91D magnesium alloy using ANOVA in ball burnishing process. Turkish Journal of Engineering, 1(1), 25–31. https://doi.org/10.31127/tuje.316860